ACS chemical biology

Articles

pubs.acs.org/acschemicalbiology

A Glycosylated, Labionin-Containing Lanthipeptide with Marked Antinociceptive Activity

Marianna Iorio,[†,∥] Oscar Sasso,[‡,∥] Sonia I. Maffioli,[†] Rosalia Bertorelli,[‡] Paolo Monciardini,[†] Margherita Sosio,[†] Fabiola Bonezzi,[‡] Maria Summa,[‡] Cristina Brunati,[†] Roberta Bordoni,[§] Giorgio Corti,[§] Glauco Tarozzo,[‡] Daniele Piomelli,[‡] Angelo Reggiani,*[,‡] and Stefano Donadio*[,†]

[†]NAICONS Srl, Via Fantoli 16/15, 20138 Milano, Italy

[‡]Department of Drug Discovery and Development, Italian Institute of Technology, Via Morego 30, 16163 Genova, Italy

[§]Institute of Biomedical Technologies, National Research Council, Via Fratelli Cervi 93, 20090 Segrate, Italy

Supporting Information

ABSTRACT: Among the growing family of ribosomally synthesized, post-translationally modified peptides, particularly intriguing are class III lanthipeptides containing the triamino acid labionin. In the course of a screening program aimed at finding bacterial cell wall inhibitors, we discovered a new lanthipeptide produced by an *Actinoplanes* sp. The molecule, designated NAI-112, consists of 22 amino acids and contains an N-terminal labionin and a C-terminal methyl-labionin. Unique among lanthipeptides, it carries a 6-deoxyhexose moiety *N*-linked to a tryptophan residue. Consistently, the corresponding gene cluster encodes, in addition to the LanKC enzyme characteristic of this lanthipeptide class, a glycosyl transferase. Despite possessing weak antibacterial activity, NAI-112 is effective in experimental models of nociceptive pain, reducing pain symptoms in mice in both the formalin and the chronic constriction injury tests. Thus, NAI-112 represents, after the labyrinthopeptins, the second example of a lanthipeptide effective against nociceptive pain.

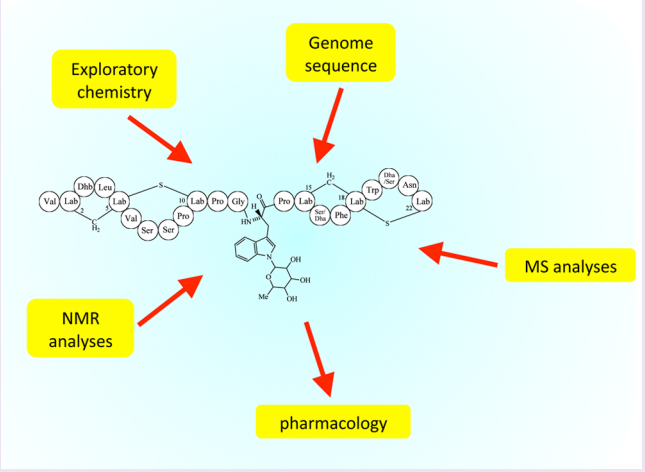

Ribosomally synthesized, post-translationally modified peptides constitute a growing family of microbially synthesized compounds endowed with unique structural features.[1] Among them, one of the best known groups is represented by the lanthipeptides, characterized by lanthionine (Lan) residues in which thioether bridges link cysteine and serine/threonine residues.[2] Most of the lanthionine-containing peptides are also known as lantibiotics (e.g., nisin), since they were discovered through bioactivity-based screens for their antibacterial activities.[3,4]

Lanthipeptides are currently divided into four classes on the basis of the enzyme(s) responsible for installing the lanthionine bridges.[1] Among them, class III lanthipeptides are made by enzymes designated as LanKC, possessing an N-terminal lyase domain, a central Ser/Thr kinase domain, and a C-terminal cyclase domain.[5−7] Particularly intriguing is the observation that some class III lanthipeptides, but not all, contain the unusual triamino acid labionin (Lab), which results from cyclodehydration of two serine and one cysteine residues in a mechanism similar to that used for lanthionine formation. In this case, however, the enolate intermediate is not quenched by protonation but undergoes a second Michael addition *in situ* with a second dehydroalanine, yielding the characteristic quaternary carbon of Lab residues. Since the discovery of the labyrinthopeptins, the first Lab-containing lanthipeptides,[8] this unusual amino acid has been found in few other lanthipeptides.[9,10]

In the course of a screening program for peptidoglycan inhibitors, we unexpectedly discovered a labionin-containing lanthipeptide, designated NAI-112, which possesses unique structural properties. Since labyrinthopeptins have been reported to exert potent antiallodynic effects in the spinal nerve injury model of neuropathic pain,[11] we also assessed whether NAI-112 has antinociceptive/antiallodynic activity in two different experimental models of inflammatory pain.

RESULTS AND DISCUSSION

Discovery of NAI-112. As part of a systematic evaluation of fermentation broth extracts fulfilling the selection criteria for cell wall inhibitors in a phenotypic screen (growth inhibition of

Received: September 9, 2013
Accepted: November 5, 2013
Published: November 5, 2013

   dx.doi.org/10.1021/cb400692w | *ACS Chem. Biol.* 2014, 9, 398−404

a *Staphylococcus aureus* strain; no inhibition of its isogenic L-form; and no reversion of antibacterial activity after incubation with either β-lactamases or excess D-alanyl-D-alanine),[11,12] one extract, derived from *Actinoplanes* DSM24059, produced an active peak **1**, designated as NAI-112, along with minor amounts of the related compound **2** (Figure 1). Under the best

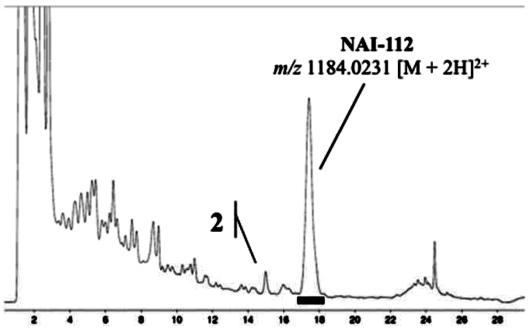

Figure 1. HPLC fractionation of the *Actinoplanes* DSM24059 extract. Eluent was monitored at 270 nm. The HPLC fractions inhibiting growth of *S. aureus* are indicated by a black bar.

conditions identified so far, NAI-112 production started during exponential growth and reached a maximum at ca. 120 mg mL^{-1}, in coincidence with the end of the growth phase (Supplementary Figure S1).

Structure Elucidation of NAI-112. High-resolution MS of **1** (Supplementary Figure S2A) pointed to the formula $C_{109}H_{147}N_{25}O_{31}S_2$ (calcd 1184.0146 $[M + 2H]^{2+}$; found 1184.0231 $[M + 2H]^{2+}$). Upon hydrolysis, the amino acids Gly, Trp, Ser, Pro, Val, Leu, and Phe were identified in the approximate ratio 1:2:3:3:2:1:1. Amidation with benzylamine and reaction with PhNCS indicated the presence of one free carboxylic acid and one amino group, respectively. Edman degradation stopped at the first cycle after Val elimination. The easy loss of 146 amu upon acid treatment, which transformed **1** into a more hydrophobic species, together with acetonide formation observed with the intact molecule, suggested the presence of a sugar moiety. Lack of reactions with dithiothreitol and iodoacetamide[13] indicated the absence of disulfides and free cysteines, whereas the different reactivity observed with ethanethiol (EtSH) at basic[14] and neutral[15] pH indicated the presence of two thioethers. However, the many overlapping signals observed in the NMR spectrum of **1** prevented structure elucidation.

Luckily, partial hydrolysis of **1** afforded a small amount of compound **3** with *m/z* 1098 $[M + H]^+$, whose NMR spectra (Supplementary Figures S3–S5) indicated the presence of the peptide sequence Val-X-Dhb-Leu-X-Val-Ser-Ser-Pro-X-Pro-Gly, where X and Dhb designate lanthionine-like and dehydrobutyrine residues, respectively (Supplementary Table S1). This sequence was then used to query a draft genome of *Actinoplanes* DSM24059, leading to the identification of a 43-aa Coding DNA Sequence (CDS) that included the segment established by NMR as VSTLSVSSPCPG, preceded by a 21-aa leader and followed by 10 further residues. Furthermore, this CDS lies within a locus with genes typical of class III lanthipeptides (Figure 2A).

The 22-aa sequence predicted from genomic data was then used as a template to interpret the MS^n (Supplementary Figure S2B) and NMR data (Supplementary Figures S6–S8) of **1**. The presence in the MS^n of the glycosylated [1–13]-fragment and

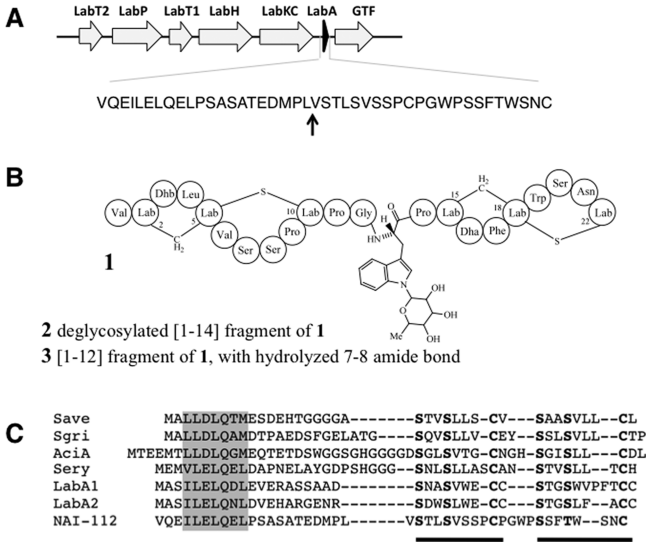

Figure 2. NAI-112, its gene cluster and Lab-containing lanthipeptides. (A) Cluster organization with detail of the precursor peptide. The arrow denotes the site of processing of the precursor peptide. (B) Schematic structure of NAI-112 and of the related compounds **2** and **3**. (C) Correlation among precursor peptides of Lab-containing class III lanthipeptides. Residues involved in (Me)Lab formation are in bold type, with each (Me)Lab ring indicated by a black bar. Precursor peptides are the labyrinthopeptins, from *Streptomyces griseus* (Sgri), *Streptomyces avermitilis* (Save), and *Saccharopolyspora erythraea* (Sery) and from *Catenulispora acidiphila* (AciA).

of an unmodified [11–22]-fragment indicated that the sugar should reside between Pro11 and Trp13 (Supplementary Figure S2B), while NMR analyses established that the sugar, a 6-deoxyhexose, is anomerically linked to the indole nitrogen of Trp13. The NMR data are fully consistent with the amino acid sequence predicted from the genome sequence, indicating also the presence of Dhb3 and Dha16 (dehydroalanine) residues. Except for the three Pro and the two Trp residues that showed partially overlapping signals, the assignments of the other amino acid spin systems were mostly complete (Supplementary Table S1). The observed chemical shifts are in agreement with the values expected for a Lab residue involving positions 2-5-10 and a methyl-labionin (MeLab) involving positions 15-18-22 (Figure 2B). Particularly, the Lab and MeLab residues assignments represent the first such description: the proton signals are similar to those of Lan residues, while the characteristic quaternary carbon of the central Lab residue is clearly discernible at 61.5 ppm in compound **3** (Supplementary Table S1).

In conclusion, the structural data indicate that NAI-112 is a 22-aa, neutrally charged, glycosylated lanthipeptide containing N-terminal Lab and C-terminal MeLab residues separated by a 4-aa linker (Figure 2B). Each series of rings contains both dehydrated and unmodified Ser residues (Figure 2B). On the basis of MS data, compound **2** likely represents the deglycosylated [1–14] N-terminal segment of NAI-112 (Figure 2B). NAI-112 represents the first occurrence of a lanthipeptide containing a MeLab and an *N*-glycosylation. While *N*-glycosylindoles are encountered in microbial [e.g., staurosporins,[16] rebeccamycins,[17] and neosidomycin[18]] and plant [e.g., vincosamides[19]] metabolites, we are unaware of any natural product containing an *N*-glycosylated Trp residue. To our knowledge, the closest example is represented by chorion

dx.doi.org/10.1021/cb400692w | ACS Chem. Biol. 2014, 9, 398–404

peroxidase from the mosquito *Aedes aegypti*, the main vector of dengue and yellow fever, in which α-D-mannose is covalently connected via the N-1 atom of the indole ring.[20,21]

NAI-112 Gene Locus. The *Actinoplanes* DSM24059 locus includes seven genes likely involved in NAI-112 biosynthesis. The structural gene *labA* encodes a leader peptide with the ILELQE motif (Figure 2C), highly conserved in class III precursor peptides and essential for enzymatic processing.[22] Upstream to *labA* are *labKC*, coding for the expected Ser/Thr kinase, lyase, and cyclase domains; *labH*, *labT1*, and *labT2*, coding for ABC transporters with putative immunity and secretion functions; and *labP*, encoding an aminopeptidase possibly involved in the leader peptide processing, which however does not show obvious relatedness to other lanthipeptide-associated proteases (Figure 2A). Consistent with NAI-112 being produced in a glycosylated form, a glycosyltransferase-encoding gene lies downstream to *labA*. As expected, the LabA core peptide contains the characteristic Ser/Ser/Cys and Ser/Thr/Cys motifs that serve as precursors for Lab and MeLab formation, respectively (Figure 2C).

In addition to the labyrinthopeptins and catenulipeptin, NAI-112 represents the third example of a lanthipeptide that is produced exclusively in (Me)Lab-containing form. This finding may help shed light on the role of the precursor peptide and/or the LabKC enzyme in directing post-translational modifications toward Lan or Lab.

Antibacterial Activity. The purified compound shows only modest antibacterial activity, with MIC values of 32−64 μg mL^{-1} against staphylococci and streptococci at standard inocula (10^5 CFU mL^{-1}). Under the conditions of the screening assay [10^4 CFU mL^{-1} and 18-h incubation],[11] an impact on *S. aureus* growth could however be observed at 4−8 μg mL^{-1} (Supplementary Figure S9), consistent with the screening data, which indicated the presence of a single antibacterial activity in the original extract (Figure 1). However, such a weak antibacterial activity is in stark contrast with the properties of many lantibiotics[23,24] and suggested that NAI-112 may possess additional activities.

Among the few Lab-containing lanthipeptides, in only two cases have data on bioactivity been reported: catenulipeptin lacks antibacterial activity but is able to restore aerial growth to surfactin-treated mycelium of *Streptomyces coelicolor*;[10] and labyrinthopeptin A2 possesses moderate antiviral activity but is highly active in a neuropathic pain model.[8] Despite possessing unrelated amino acid sequences and unique structural features, NAI-112 and labyrinthopeptin A2 share a similar ring topology (Figure 2C). We thus tested NAI-112 in experimental models of neuropathic pain.

Antinociceptive Activity. We initially tested NAI-112's ability to prevent pain-related behaviors elicited in mice by intraplantar injection of the chemical irritant formalin. The formalin test is a tonic model of continuous pain resulting from tissue injury. The first phase has been associated to acute nociceptive pain, while the second phase should mimic a more tonic (chronic) state. Systemic administration of NAI-112 (1−10 mg kg^{-1}, i.p.) caused a dose-dependent reduction of formalin-induced pain behavior (Figure 3A). Substantial activity was observed on both the first phase of formalin pain, which involves acute activation of sensory C fibers, and the second phase of formalin pain, in which sensory fibers activity is accompanied by inflammation and central sensitization. Similar effects were observed when NAI-112 (1−100 μg per animal) was injected into the hind paw together with formalin (Figure 3B). Also compound **2** tested at 10 mg kg^{-1} i.p. was effective in the formalin test, with efficacy comparable to that of NAI-112 (Figure 3C), although the effect on the second phase of formalin pain was less pronounced. When tested at 10 mg kg^{-1}, i.p., on the Rotarod assay, NAI-112 did not interfere with motor coordination up to 60 min after administration (Figure 4). Furthermore, in a separate set of animals, mice treated with NAI-112 at 30 μg/10 μL, i.c.v., displayed normal behavior and no sign of toxicity up to 48 h.

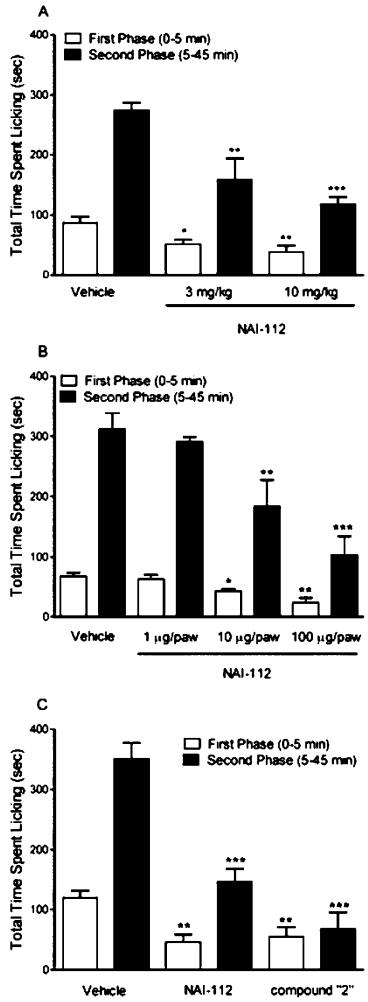

Figure 3. Formalin test in mice. Antinocifensive effect of NAI-112 on early (0−15 min) or late (15−45 min) phases after intraperitoneal injection (3−10 mg kg^{-1}) (A) and intraplantar injection (1−100 μg/paw) (B). Effect of intraperitoneal injection of compound **2** (10 mg kg^{-1}) (C). Animals (n = 6) were immediately transferred to a transparent observation chamber, where nocifensive behavior (time spent licking and biting the injected paw) was continuously monitored for 45 min. Nocifensive response is expressed as mean ± SEM. Symbols indicate statistical significance as * $p < 0.05$, ** $p < 0.01$, and *** $p < 0.001$ vs vehicle.

Interestingly, the first phase of the antinociceptive effect of 10 mg kg^{-1} i.p. NAI-112 in the formalin test was prevented by the administration of AMG9810, a selective TRPV1 antagonist,[25] whereas no prevention was seen with the CB_1 inverse agonist AM251 (Figure 5A),[26] the opioid antagonist naloxone, or the α2 adrenergic antagonist yohimbine (Figure 5B). Thus, while NAI-112 is effective on both phases, indicating a broad antinociceptive efficacy, the first phase of antinociceptive effect can be prevented by a selective TRPV1 antagonist.

dx.doi.org/10.1021/cb400692w | ACS Chem. Biol. 2014, 9, 398−404

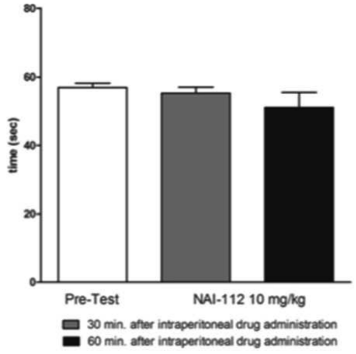

Figure 4. Motor coordination after NAI-112 injection. The time spent by animals on the Rotarod was recorded 30 and 60 min after NAI-112 administration and expressed in seconds as mean ± SEM. Control animals received i.p. vehicle (10% PEG, 10% Tween 80 in saline).

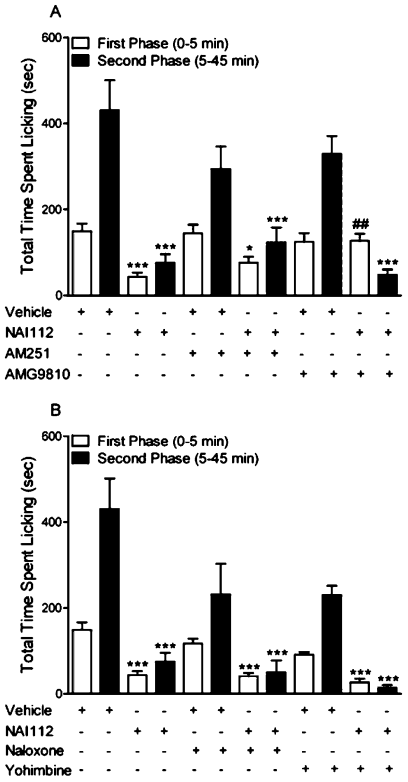

Figure 5. Antinocifensive effect of NAI112 in the formalin test was challenged with the selective TRPV1 antagonist AMG9810 (1 mg kg^{-1}; i.p.) and the CB1 inverse agonist AM251 (5 mg kg^{-1}; i.p.) (A) or the $\alpha 2$ antagonist yohimbine (5 mg kg^{-1}; i.p.) and the opioid antagonist naloxone (1 mg kg^{-1}; i.p.) (B). The antagonists were injected 30 min before formalin challenge. Animals (n = 6) were immediately transferred to a transparent observation chamber, where nocifensive behavior (time spent licking and biting the injected paw) was continuously monitored for 45 min. Nocifensive response is expressed as mean ± SEM. Symbols indicate statistical significance as * $p < 0.05$, ** $p < 0.01$, and *** $p < 0.001$ vs vehicle; and ## $p < 0.01$ vs NAI-112.

NAI-112 was then studied for its ability to alleviate established chronic pain condition. The compound was tested in the sciatic nerve chronic constriction injury (CCI) model of persistent hyperalgesia and allodynia in mice, a model that has both inflammatory and neuropathic pain components. NAI-112 (3, 10, and 30 mg kg^{-1}, i.p.) was administered on day 7 after left sciatic nerve ligation, and pain readouts were measured 2 h after dosing. As shown in Figure 6, a single administration of

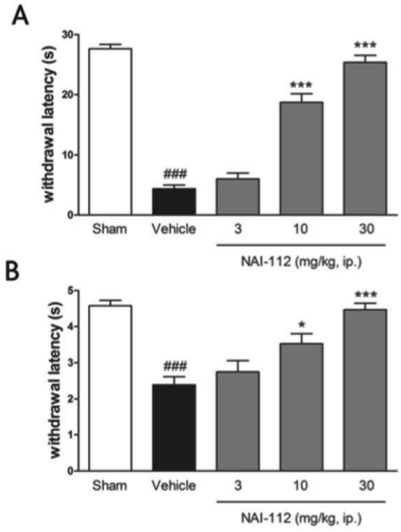

Figure 6. Effect of NAI-112 in the CCI model. Intraperitoneal injection of NAI-112 (1−30 mg kg^{-1}) reduced both heat hyperalgesia (A) and mechanical allodynia (B). Hyperalgesia and allodynia were measured 2 h after treatment. Results are expressed as mean ± SEM (n = 6, each group). *** $p < 0.001$ vs vehicle; ### $p < 0.001$ vs sham-operated mice.

NAI-112 was sufficient to reduce significantly both hyperalgesia (Figure 6A) and allodynia (Figure 6B) in a dose-dependent manner, with a full effect at 30 mg kg^{-1}. NAI-112 is also effective on an established chronic pain state such as the CCI model, and thus our findings indicate that the antinociceptive profile of NAI-112 could be further expanded to chronic mixed inflammatory/neuropathic pain states.

The mechanism by which NAI-112 modulates pain behavior is unclear. Our findings indicate that NAI-112 does not act through opioid, cannabinoid, or descending adrenergic mechanisms. Interestingly, in the first phase of formalin assay the effect of NAI-112 was sensitive to nonanalgesic doses of the TRPV1 antagonist AMG9810, suggesting an engagement of the vanilloid pathway. However, NAI-112 has no TRPV1 antagonistic activity *in vitro* (by binding assay; data not shown), and thus NAI-112 might act, at least partially, via an as-yet unidentified mechanism on a vanilloid-sensitive pathway.

Conclusions. NAI-112 shares antiallodynic activities with labyrinthopeptins and natural peptides from spider toxins or cone snails. Although a direct comparison of the bioactivities of NAI-112 and labyrinthopeptins is not possible, since different animal models and route of administrations were used, it is striking that two lanthipeptides, unrelated in their amino acid sequence, exert similar bioactivities *in vivo*. Furthermore, the observation that the N-terminal portion of NAI-112 retains some activity in the formalin test is reminiscent of the mechanism of action of nisin and related lantibiotics. In that case, the two N-terminal rings are involved in binding to the lipid II target, while the C-terminal portion of the lantibiotic determines further events after this initial docking step.[23] In any case, the results presented here suggest that lanthipeptides possess interesting bioactivities beyond their well-established properties as antibacterial agents. This finding highlights the

dx.doi.org/10.1021/cb400692w | *ACS Chem. Biol.* 2014, 9, 398−404

possibility of further exploring this class of microbial metabolites as drug leads for pain-related applications.

METHODS

Analytical Procedures. LC−MS was performed on an Agilent 1100 series liquid chromatograph equipped with an Ascentis express Supelco RP18, 2.7 μm (50 mm × 4.6 mm) column eluted at 1 mL min^{-1} at 40 °C using a multistep program: time = 0 (5% phase B); time = 6 min (95% phase B); time = 7 min (100% phase B); phases A and B were 0.05% (v/v) TFA in H_2O and CH_3CN, respectively. The column effluent was split 50:50 with one part diverted to a photodiode array detector and the other to the ESI interface of a Bruker Esquire3000 plus ion trap mass spectrometer, set as follows: sheat gas (N_2) at 50 psi, dry gas at 10 L min^{-1}, capillary heater at 365 °C, positive polarity and −4000 V capillary voltage (sample inlet conditions); −500 V as end plate offset; 200 ms maximum ion time, 5 ms ion time, 5 ms; scan 3 full micro, duration 10 min segment duration, and 100−2400 *m/z* scan events.

LC−HRMS analyses were performed on a Surveyor Accela HPLC system (Thermo Fisher Scientific) connected to an Exactive benchtop mass spectrometer (Thermo Fisher Scientific), equipped with a NSI-ESI ion source. Samples were injected on a C8 reversed phase column (BioBasic C8, 100 mm × 0.18 mm, 5 μm, 300A, Thermo Fisher Scientific) and eluted with the following gradient: 5% phase B_2 for 3 min, 5% to 65% B_2 in 17 min, and 65% to 95% B_2 in 5 min (eluents A_2 and B_2 were 0.1% formic acid in H_2O and CH_3CN, respectively); the flow rate was 100 μL min^{-1} split in order to achieve a final flux of 2 μL min^{-1}.

HPLC analyses were performed using an LC 2010A-HT liquid chromatograph (Shimadzu Corporation) equipped with a LiChrosphere C18 5 μm, 4.6 mm × 100 mm column (Merck). Elution was performed at 1 mL min^{-1}, 50 °C with a linear gradient from 10% to 90% phase B_3 in 30 min. Phases A_3 was 0.1% TFA (v/v) in H_2O and phase B_3 was CH_3CN. UV detection was set at 230 and 270 nm.

^{1}H,^{13}C and 1- and 2-D NMR spectra (COSY, TOCSY, HSQC, HMBC) were measured in CD_3CN/H_2O (6:4) at 298 K using an AMX 600 MHz spectrometer (Bruker). Proton and carbon chemical shifts were referenced to the residual solvent signal (CD_3CN) at 1.94 and 1.32 ppm, respectively. Two-dimensional experiments including TOCSY, COSY, HMQC, and HMBC were performed using Bruker standard pulse sequences. Data were processed with WIN NMR software (Bruker).

***Actinoplanes* Cultivation.** *Actinoplanes* sp. DSM24059 was classified as *Actinoplanes* on the basis of its almost complete 16S rRNA gene sequence, determined as described.[27] The strain was cultivated in 500-mL Erlenmeyer flasks containing 100 mL of seed medium (10 g L^{-1} dextrose monohydrate, 24 g L^{-1} maize dextrin, 5 g L^{-1} yeast extract, 5 g L^{-1} soya peptone, pH 7.2). After 72 h at 30 °C, 100 mL was inoculated into 2 L of production medium [10 g L^{-1} dextrose monohydrate, 10 g L^{-1} maltose, 4 g L^{-1} yeast extract, 12 g L^{-1} Pharmamedia (Traders Protein), 4 g L^{-1} $CaCO_3$, pH 7.3]. The strain was grown at 30 °C with 600 rpm stirring and 0.5 vvm aeration in a BioFlo 115 bioreactor (New Brunswick Scientific), maintaining pH at <6.8 by addition of 5% sulphuric acid. Strain growth was measured as packed mycelial volume (PMV%) by centrifuging a 5-mL culture in a graduated tube for 10 min at 1800 rcf in a swinging bucket centrifuge. Production of NAI-112 was monitored by HPLC, after the culture was extracted with two volumes of methanol for 1 h at 50 °C.

NAI-112 Recovery and Purification. The culture (2 L) was mixed with 2 L of methanol, shaken for 2 h at RT, and centrifuged at 3000 rpm for 10 min. The supernatant, evaporated to a reduced volume (500 mL), was extracted twice with 250 mL of butanol. The combined organic phases were evaporated to dryness under vacuum, dissolved in DMF/H_2O 1:1, and purified by medium pressure chromatography on 86 g of reverse phase C18 RediSep RF column (40−63 μm particle size, 60 Å pore size, 230−400 mesh) using a CombiFlash RF Teledyne Isco Medium Pressure Chromatography System. The resin was previously conditioned at 60 mL min^{-1} with a mixture of phase A_3:phase B_3 9:1 (v/v), brought to 30% phase B_3 in 1 min and eluted with a 14-min linear gradient from 30% to 55% phase B_3. The fractions containing NAI-112 were pooled, concentrated under vacuum, and lyophilized, yielding 182 mg of NAI-112. During chromatography, 2.4 mg of compound **2** (HPLC retention time 14.3 min, *m/z* 1362 $[M + H]^+$) was also recovered.

Explorative Chemistry. *Amino Acid Analyses.* Compound **1** (3 mg), hydrolyzed in 1 mL of 6 M HCl at 160 °C for 5 min under microwave irradiation, was evaporated to dryness, resuspended in 1 mL of H_2O/CH_3CN 1:1, adjusted to pH 7.0 with triethylamine and treated with (*R*)-(−)-NBD-PyNCS (5 mg). The reaction mixture was stirred for 2 h at 60 °C and then extracted twice with 3 mL of petroleum ether/CH_2Cl_2 8:2. The organic phase was evaporated to dryness, redissolved in 1 mL of H_2O/CH_3CN 1:1 and analyzed by HPLC−MS.

Reaction with PhNCS. Compound **1** (7 mg) was dissolved in 200 μL of DMF, and 10 μL of TEA and 2 μL of PhNCS were added. After stirring at RT for 1 h, complete transformation was observed into a 4.9-min lipophilic peak with *m/z* 1254.2 $[M + 2H]^{2+}$. After evaporation to dryness the residue was resuspended in 500 μL of water and extracted with CH_2Cl_2/hexane 2:8 (2 × 2 mL). The aqueous phase was dried, dissolved in 50% TFA, and kept for 1 h at RT, when LC−MS showed the presence of *m/z* 1134.9 $[M + 2H]^{2+}$ and 1062.4 $[M + 2H]^{2+}$, corresponding to the Edman product after N-terminal Val removal with and without the sugar moiety, respectively.

Amidation. Compound **1** (7 mg) was dissolved in 200 μL of DMF, added to 50 μL of *N*,*N*-dimethylethylenediamine to pH 7 (pH tested after dilution 1:10 in H_2O), and reacted with PyBOP (5 mg) for 30 min at RT, when LC−MS analysis showed the formation of monoamidated compound with *m/z* 1218.7 $[M + 2H]^{2+}$.

Reaction with EtSH at pH 11. Compound **1** (7 mg) was dissolved in 200 μL of DMF and added to 200 μL of a solution consisting of 780 μL of EtOH, 560 μL of H_2O, 180 μL of 5 M NaOH, and 168 μL of EtSH. The mix was reacted for 2 h at 60 °C, when a peak was observed with *m/z* 1276.7 $[M + 2H]^{2+}$, corresponding to addition of three EtSH molecules.

Reaction with EtSH at pH 7. Compound **1** (3 mg) was dissolved in 400 μL of MeCN and 400 μL of 0.1 M acetate buffer, pH 7. EtSH (3 μL) was added, and the solution allowed to react at 50 °C for 1 h, when a peak was observed with *m/z* 1215.8 $[M + 2H]^{2+}$, corresponding to addition of one EtSH.

Acetonide Formation. Compound **1** (33 mg) was dissolved in 2 mL of DMF/acetone 1:9. *p*-Toluenesulfonic acid (5 mg) was added, and the solution was stirred for 5 h at 45 °C, when a peak was observed having *m/z* 1204.6 $[M + 2H]^{2+}$. After solvent evaporation the residue was purified by medium pressure reversed chromatography, as above. NMR analysis of the purified compound showed a quaternary carbon at 110 ppm expected from a 1,2 diol acetonide derivative.

Partial Hydrolysis. Compound **1** (50 mg) was dissolved in 50% TFA and allowed to react for one week at 40 °C. After evaporation, the main hydrolysis product **3** (*m/z* 1098 $[M + H]^+$) was purified by medium pressure liquid chromatography as above.

Genome Sequence and Identification of the NAI-112 Gene Cluster. High molecular weight gDNA was prepared from *Actinoplanes* sp. DSM24059 grown in seed medium for 4 days. A draft genomic sequence was generated by the 454 technology, which yielded 1900 contigs for a total of 7.4 Mb. A CDS encoding the peptide sequence deduced from NMR data was found in a 10590-nt contig, which was then connected on the right-end side of Figure 2A to a 3350-nt contig by targeted PCR.

***In Vitro* Assays.** MICs were determined by broth microdilution as described.[12] Growth curves were measured using a 5×10^4 CFU mL^{-1} inoculum of *S. aurues* L100 in a 96-well microtiter plate, which was incubated at 37 °C in a Synergy 2 plate reader (BioTek) recording the optical densities at 595 nm (OD_{595}) over 20 h. Binding assays were performed by CEREP Sa.

Animals. Male CD1 mice weighing 25−30 g (Charles River) were used in accordance with the Ethical Guidelines of the International Association for the Study of Pain and in compliance with Italian and European Economic Community regulations (D.M. 116192; O.J. of

dx.doi.org/10.1021/cb400692w | ACS Chem. Biol. 2014, 9, 398−404

E.C. L 358/1 12/18/1986). Mice were housed in groups of 5 or 4, in ventilated cages containing autoclaved cellulose paper as nesting material, with free access to food and water. They were maintained under a 12-h light/dark cycle (lights on at 08:00 a.m.), at controlled temperature (21 ± 1 °C) and relative humidity (55 ± 10%). Behavioral testing was performed between 9:00 a.m. and 5:00 p.m.

Mouse Formalin Test. Ten microliters of 5% formalin was injected into the plantar surface of the left hind paw, and the time the animals spent licking the injected paw was measured. As expected, two distinct periods of high licking activity were identified, an early phase lasting the first 5 min and a late phase lasting from 15 to 45 min after formalin injection. Nocifensive behavior was monitored (licking and biting of the injected paw) for 45 min in blocks of 5 min each. Compounds were dissolved in 10% PEG400/10% Tween 80 and 80% saline and administered intraperitoneally at 1, 3, and 10 mg kg^{-1}, 30 min before formalin injection.

Chronic Constriction Injury (CCI). Sciatic nerve ligations were performed as described.[28] Adult male CD1 mice were anesthetized with 2−3% isoflurane, and the left sciatic nerve was exposed at midthigh level through a small incision and tied at two distinct sites (spaced at a 2-mm interval) with a silk thread. The wound was closed with a single muscle suture and skin clips and dusted with streptomycin. In sham-operated animals, the nerve was exposed but not tied. All experiments were performed in a quiet room by scientists unaware of the treatment protocol at the time of the test (blind procedure). Thermal hyperalgesia was assessed as described,[29] measuring the latency to withdraw the hind paw from a focused beam of radiant heat (thermal intensity: infrared 3.0) applied to the plantar surface using a plantar test apparatus (Ugo Basile). The cutoff time was set at 30 s. Withdrawal latency was measured on the injured ipsilateral paw.

For the measurement of tactile allodynia with the Von Frey dynamic plantar aesthesiometer (DPA), animals were placed individually in a small enclosed testing arena (20 cm × 18.5 cm × 13 cm) with a wire mesh floor for 5 min. The DPA device was positioned beneath the animal, so that the filament was directly under the plantar surface of the paw to be tested. When a trial was started, the device raised the filament to touch the paw and progressively increased force until the animal withdrew its paw, or until it reached a maximum of 5 g of force. The DPA automatically records the force at which the paw is withdrawn and the withdrawal latency (latency and maximum force are directly related, because the device progressively increases force until withdrawal occurs). Compounds were dissolved and administered as above. Pain behavior was measured 2 h after dosing.

■ ASSOCIATED CONTENT

Ⓢ Supporting Information

NMR and MS spectral data for NAI-112, fermentation time course, and antibacterial activities. This material is available free of charge via the Internet at http://pubs.acs.org.

Accession Codes

The DNA sequence of the 16S rRNA gene and the NAI-112 gene cluster from *Actinoplanes* sp. DSM24059 have been submitted to GenBank with accession numbers KF438031 and KF765778, respectively.

■ AUTHOR INFORMATION

Corresponding Authors

*E-mail: angelo.reggiani@iit.it

*E-mail: sdonadio@naicons.com

Author Contributions

‖These authors contributed equally to this work.

Notes

The authors declare the following competing financial interest(s): M.I., O.S., S.I.M., R. Bertorelli, P.M., M.S., A.R., and S.D. are co-inventors of a patent application on NAI-112 derivatives filed by Naicons and IIT. The intellectual property rights linked to the patent applications are owned by Naicons and IIT. M.I., S.I.M., P.M., M.S., and S.D. are employees of Naicons and own shares of Naicons.

■ ACKNOWLEDGMENTS

This work was partially supported by grants to NAICONS from Regione Lombardia and from the European Commission (contract number 245066 for FP7-KBBE-2009-3).

■ REFERENCES

(1) Arnison, P. G., Bibb, M. J., Bierbaum, G., Bowers, A. A., Bugni, T. S., Bulaj, G., Camarero, J. A., Campopiano, D. J., Challis, G. L., Clardy, J., Cotter, P. D., Craik, D. J., Dawson, M., Dittmann, E., Donadio, S., Dorrestein, P. C., Entian, K. D., Fischbach, M. A., Garavelli, J. S., Göransson, U., Gruber, C. W., Haft, D. H., Hemscheidt, T. K., Hertweck, C., Hill, C., Horswill, A. R., Jaspars, M., Kelly, W. L., Klinman, J. P., Kuipers, O. P., Link, A. J., Liu, W., Marahiel, M. A., Mitchell, D. A., Moll, G. N., Moore, B. S., Müller, R., Nair, S. K., Nes, I. F., Norris, G. E., Olivera, B. M., Onaka, H., Patchett, M. L., Piel, J., Reaney, M. J., Rebuffat, S., Ross, R. P., Sahl, H. G., Schmidt, E. W., Selsted, M. E., Severinov, K., Shen, B., Sivonen, K., Smith, L., Stein, T., Süssmuth, R. D., Tagg, J. R., Tang, G. L., Truman, A. W., Vederas, J. C., Walsh, C. T., Walton, J. D., Wenzel, S. C., Willey, J. M., and van der Donk, W. A. (2013) Ribosomally synthesized and post-translationally modified peptide natural products: overview and recommendations for a universal nomenclature. *Nat. Prod. Rep. 30*, 108−160.

(2) Knerr, P. J., and van der Donk, W. A. (2012) Discovery, biosynthesis, and engineering of lantipeptides. *Annu. Rev. Biochem. 81*, 479−505.

(3) Willey, J. M., and van der Donk, W. A. (2007) Lantibiotics: peptides of diverse structure and function. *Annu. Rev. Microbiol. 61*, 477−501.

(4) Maffioli, S. I., Monciardini, P., Sosio, M., and Donadio, S. (2012) New lantibiotics from natural and engineered strains. In *Drug Discovery from Natural Products* (Genilloud, O., and Vicente, F., Eds.), pp 116−139, RSC Publishing, Cambridge, U.K.

(5) Kodani, S., Hudson, M. E., Durrant, M. C., Buttner, M. J., Nodwell, J. R., and Willey, J. M. (2004) The SapB morphogen is a lantibiotic-like peptide derived from the product of the developmental gene *ramS* in *Streptomyces coelicolor*. *Proc. Natl. Acad. Sci. U.S.A. 101*, 11448−11453.

(6) Goto, Y., Li, B., Claesen, J., Shi, Y., Bibb, M. J., and van der Donk, W. A. (2010) Discovery of unique lanthionine synthetases reveals new mechanistic and evolutionary insights. *PLoS Biol. 8*, e1000339.

(7) Müller, W. M., Schmiederer, T., Ensle, P., and Süssmuth, R. D. (2010) In vitro biosynthesis of the prepeptide of type-III lantibiotic labyrinthopeptin A2 including formation of a C-C bond as a post-translational modification. *Angew. Chem., Int. Ed. 49*, 2436−2440.

(8) Meindl, K., Schmiederer, T., Schneider, K., Reicke, A., Butz, D., Keller, S., Gühring, H., Vértesy, L., Wink, J., Hoffmann, H., Brönstrup, M., Sheldrick, G. M., and Süssmuth, R. D. (2010) Labyrinthopeptins: a new class of carbacyclic lantibiotics. *Angew. Chem., Int. Ed. 49*, 1151−1154.

(9) Völler, G. H., Krawczyk, J. M., Pesic, A., Krawczyk, B., Nachtigall, J., and Süssmuth, R. D. (2012) Characterization of new class III lantibiotics-erythreapeptin, avermipeptin and griseopeptin from *Saccharopolyspora erythraea, Streptomyces avermitilis* and *Streptomyces griseus* demonstrates stepwise N-terminal leader processing. *ChemBioChem. 13*, 1174−1183.

(10) Wang, H., and van der Donk, W. A. (2012) Biosynthesis of the class III lantipeptide catenulipeptin. *ACS Chem. Biol. 7*, 1529−1535.

(11) Jabes, D., and Donadio, S. (2010) Strategies for the isolation and characterization of antibacterial lantibiotics. *Methods Mol. Biol. 618*, 31−45.

(12) Simone, M., Monciardini, P., Gaspari, E., Donadio, S., and Maffioli, S. I. (2013) Isolation and characterization of NAI-802, a new

lantibiotic produced by two different *Actinoplanes* strains. *J. Antibiot. 66*, 73−78.
(13) Kabuki, T., Uenishi, H., Seto, Y., Yoshioka, T., and Nakajima, H. J. (2009) A unique lantibiotic, thermophilin 1277, containing disulfide bridge and two thioether bridges. *J. Appl. Microbiol. 106*, 853−862.
(14) Meyer, H. E., Heber, M., Eisermann, B., Korte, H., Metzger, J. W., and Jung, G. (1994) Sequence analysis of lantibiotics: chemical derivatization procedures allow a fast access to complete Edman degradation. *Anal. Biochem. 223*, 185−190.
(15) Smith, L., Novák, J., Rocca, J., McClung, S., Hillman, J. D., and Edison, A. S. (2000) Covalent structure of mutacin 1140 and a novel method for the rapid identification of lantibiotics. *Eur. J. Biochem. 267*, 6810−6816.
(16) Han, X.-X., Cui, C.-B., Gu, Q.-Q., Zhu, W. M., Liu, H.-B., Gu, J.-Y., and Osada, H. (2005) ZHD-0501, a novel naturally occurring staurosporine analog from *Actinomadura* sp. 007. *Tetrahedron Lett. 46*, 6137−6140.
(17) Anizon, F., Moreau, P., Sancelme, M., Voldoire, A., Prudhomme, M., Ollier, M., Sevère, D., Riou, J. F., Bailly, C., Fabbro, D., Meyer, T., and Aubertin, A. M. (1998) Synthesis, biochemical and biological evaluation of staurosporine analogues from the microbial metabolite rebeccamycin. *Bioorg. Med. Chem. 6*, 1597−1604.
(18) Furuta, R., Shunsuke, N., Tamura, A., and Yokogawa, K. (1979) Neosidomycin, a new antibiotic of *Streptomyces*. *Tetrahedron Lett. 19*, 1701−1704.
(19) Panda, S., Kar, A., Sharma, P., and Sharma, A. (2013) Cardioprotective potential of N,α-L-rhamnopyranosyl vincosamide, an indole alkaloid, isolated from the elaves of *Moringa oleifera* in isoproterenol induced cardiotoxic rats: *in vivo* and *in vitro* studies. *Bioorg. Med. Chem. Lett. 23*, 959−962.
(20) Li, J. S., Cui, L., Rock, D. L., and Li, J. (2005) Novel glycosydic linkage in *Aedes aegypti* chorion peroxidase. *J. Biol. Chem. 280*, 38513−38521.
(21) Lafite, P., and Daniellou, R. (2012) Rare and unusual glycosylation of peptides and proteins. *Nat. Prod. Rep. 29*, 729−738.
(22) Müller, W. M., Ensle, P., Krawczyk, B., and Süssmuth, R. D. (2011) Leader peptide-directed processing of labyrinthopeptin A2 precursor peptide by the modifying enzyme LabKC. *Biochemistry 50*, 8362−8373.
(23) Bierbaum, G., and Sahl, H. G. (2009) Lantibiotics: mode of action, biosynthesis and bioengineering. *Curr. Pharm. Biotechnol. 10*, 2−18.
(24) Piper, C., Cotter, P. D., Ross, P. R., and Hill, C. (2009) Discovery of medically significant lantibiotics. *Curr. Drug Discovery Technol. 6*, 1−18.
(25) Gavva, N. R., Tamir, R., Qu, Y., Klionsky, L., Zhang, T. J., Immke, D., Wang, J., Zhu, D., Vanderah, T. W., Porreca, F., Doherty, E. M., Norman, M. H., Wild, K. D., Bannon, A. W., Louis, J. C., and Treanor, J. J. (2005) AMG 9810 [(E)-3-(4-t-butylphenyl)-N-(2,3-dihydrobenzo[b][1,4] dioxin-6-yl)acrylamide], a novel vanilloid receptor 1 (TRPV1) antagonist with antihyperalgesic properties. *J. Pharmacol. Exp. Ther. 313*, 474−484.
(26) Pertwee, R. G. (2005) Inverse agonism and neutral antagonism at cannabinoid CB1 receptors. *Life Sci. 76*, 1307−1324.
(27) Mazza, P., Monciardini, P., Cavaletti, L., Sosio, M., and Donadio, S. (2003) Diversity of *Actinoplanes* and related genera isolated from an Italian soil. *Microb. Ecol. 45*, 362−372.
(28) Bennett, G. J., and Xie, Y. K. (1988) A peripheral mononeuropathy in rat that produces disorders of pain sensation like those seen in man. *Pain 33*, 87−107.
(29) Hargreaves, K., Dubner, R., Brown, F., Flores, C., and Joris, J. (1988) A new and sensitive method for measuring thermal nociception in cutaneous hyperalgesia. *Pain 32*, 77−88.